

A STUDY OF HERMETIC TRANSITIONS FOR MICROWAVE PACKAGES

Jong-Gwan Yook, Nihad I. Dib, Eray Yasan and Linda P. B. Katehi

Radiation Laboratory
 Department of Electrical Engineering and Computer Science
 The University of Michigan, Ann Arbor, MI 48109-2122

Abstract

Two numerical techniques, the finite difference in time domain (FDTD) and the finite element method (FEM) in frequency domain, are employed to characterize microstrip hermetic transition geometries in an effort to investigate high frequency effects. Measurements performed on these transitions compare favorably with theory. It is shown that these hermetic wall transitions may suffer from parasitic parallel plate modes which however can be eliminated with the use of vias at appropriate locations. Two different transitions have been analyzed from 5 GHz to 25 GHz and have been found to be limited in performance by higher return loss as frequency increases. This indicates the need for very careful characterization of transitions intended for use in microwave and millimeter-wave applications.

1 Introduction

Hermetic packages are frequently encountered in microwave integrated circuits for sealing and isolating parts of the circuitry. While hermetic packages should provide physical protection from hostile environments in addition to shielding against electromagnetic interference, they should also be electrically transparent to the circuit they protect. In the past, package design was performed to ensure good thermal and mechanical properties but very little considerations were given to electrical performance. As mentioned in many papers [1]-[7], with the electrical performance of the hermetic package ignored during the first circuit design cycle, circuit performance was compromised considerably due to uncontrollable packaging effects. Successful MIC and MMIC circuit design requires that the package is designed carefully to enhance circuit performance in addition to improving thermal and mechanical characteristics.

Inevitably, the circuit in a package needs to be connected to the outer world by means of an appropriate transition which takes into account the geometrical characteristics of the printed circuits and the electromagnetic field distribution around the transition. An effective transition from one transmission medium to another through a drastically changing environment, i.e., open space to cavity via the hermetic wall, can be obtained only if special care is taken to smoothly vary the guided field so that it conforms to the boundary conditions imposed by the environment. This may involve the use of different transmission line geometries whose finite lengths may limit bandwidth and increase undesired reflections away from the pass band. This limitation

in bandwidth may be intensified by high frequency effects which in addition to higher reflection loss introduce higher ohmic and parasitic loss.

In this paper, two hermetic microstrip transitions are analyzed. In both cases, transitions from an open $50\ \Omega$ microstrip line to a shielded $50\ \Omega$ microstrip line are realized through a hermetic wall in which the transmission medium takes the form of a CPW line (see Figure 4) or strip-coaxial line (see Figure 5). The finite element method (FEM) with edge-based vector basis functions and the finite difference time domain (FDTD) method are used to analyze these transitions, understand their performance limitations and investigate efficient means for optimization.

2 Theory

In this section, in view of a wealth of references, only a brief summary of the FEM and FDTD method is given.

2.1 Finite Element Method

To determine the electromagnetic fields distribution in a given space in the context of the finite element method, the weak form of Maxwell's equations is considered and solved with edge-based vector basis functions and tetrahedral sub-domain elements. The resulting final matrix equation is of very large order but the corresponding square matrix is sparse, thus, allowing for the use of appropriate iterative techniques. Usually, the number of non-zero elements in a given row or column ranges from 14 to 19 for a structured mesh. To solve sparse FEM matrix, the bi-conjugate gradient method with diagonal preconditioning has been implemented to speed up calculations and improve accuracy.

2.2 Finite Difference Time Domain Method

In order to characterize any planar discontinuity, propagation of a specific time-dependent function through the structure is simulated using the FDTD scheme. Following the time and space discretizations of the electric and magnetic field components, the FDTD equivalents of Maxwell's equations are then used to update the spatial distributions of these components at alternating half time steps. Moreover, the super-absorbing first-order Mur boundary condition is utilized to terminate the FDTD lattice at the front and back walls in order to simulate infinite lines. For one open geometry, the first-order Mur boundary condition is used on the top and side walls to simulate an open environment.

TH
4C

3 Numerical Results

3.1 Microstrip-through-CPW hermetic transition

For an effective transition through the cavity wall, the microstrip line is gradually changed into a coplanar waveguide which extends beyond each face of the hermetic wall. The employed section of the coplanar waveguide is back metallized by the ground of the microstrip line and gives rise to parallel plate waveguide modes, parasitic radiation and unwanted resonances that occur within the range of the operating frequencies. These resonances are pronounced when the structures are shielded but are considerably damped when these transitions operate in an open environment.

To understand the performance characteristics, the above hermetic transition is constructed in three steps. At first, a simple microstrip-through-CPW transition is analyzed to understand the parasitic effects introduced by the CPW section (Figure 1), then vias are introduced at appropriate locations in the grounded CPW section to eliminate the excited parallel plate modes (Figure 3). Finally, a hermetic wall is introduced to complete the transition geometry (Figure 4).

A. Transition through a CPW section

To characterize the microstrip-through-CPW transition in open environment without via holes under the CPW ground, the FDTD technique with appropriate radiation boundary conditions is used. As shown in Figure 1, the FDTD and measurement data match well. The differences between theoretical and experimental results are primarily due to conductor and dielectric losses in the measurement which are not included in the FDTD simulation.

Furthermore, Figure 2 shows the same transition in a shielded environment. Theoretical data derived by the FEM and the FDTD method reveal very strong resonances generated by the CPW section connecting the two microstrip lines. The Q of these resonances is much higher in the shielded case when compared to the open transition of Figure 1 due to lack of parasitic radiation.

B. Microstrip-through-CPW with an extended rectangular via hole grounding

To avoid excitation of parallel plate waveguide modes in the grounded CPW section, extended via holes are placed under the CPW ground planes (see Figure 3) and their effect is investigated. Analysis of this structure confirms that the extended rectangular via holes suppress unwanted resonances (Figure 3). As shown from these theoretically derived data, the performance of the microstrip-through-CPW transition structure degrades as frequency increases. Specifically, over 15 GHz it has more than 10 dB return loss.

C. Microstrip-through-CPW transition with hermetic wall

In this section, the effect of the hermetic wall on the microstrip-through-CPW transition with extended vias is investigated. The hermetic wall is formed by a ceramic material bonded on top of a metal plate which forms the upper part of the wall.

Figure 4 shows the geometrical details of the hermetic transition structure with extended via holes. The height of the ce-

ramic is equal to the substrate thickness while its relative dielectric constant is chosen to be $\epsilon_{r2} = 2.3$ in contrast to the 12.5 of the substrate. From a circuit point of view, the ceramic on top of the transmission line may alter the characteristic impedance of the line and hence the scattering parameters may change. Since there is another conducting plane on top of the ceramic, the CPW with hermetic wall can be considered as an in-homogeneously sandwiched CPW.

In Figure 4, the magnitude of the scattering parameters obtained using FEM and FDTD are compared. After placing the hermetic wall on top of the CPW section, the over all return loss has increased by 2 to 3 dB while its frequency dependency has remained unchanged. In the whole frequency region considered here from 5 GHz to 25 GHz, the return loss is less than -5 dB. However, in the low end of this frequency region, up to 13 GHz, the return loss is less than -10 dB. The effect of the hermetic wall is small as it is expected from the field distribution in the CPW structure.

3.2 Hermetic bead transition

Another type of commonly encountered feed-thru, a hermetic bead transition structure, is analyzed in this section. As shown in Figure 5, a circular coaxial line is approximated with rectangular-shaped stripline and the dimensions are determined to have 50 Ω characteristic impedance. Also, the dielectric constant of the ring is chosen as 10.8 which is the same as the substrate. The thickness of the hermetic wall and air gap spacings are chosen as 1.5 mm and 0.4 mm, respectively.

Scattering parameters are computed using FEM and FDTD and shown in Figure 5. The hermetic bead transition performed quite well in the low frequency end of the region as expected while the return loss degraded as frequency increased. Even though the geometrical factors are not optimized for better transition characteristics, the overall performance of the circuit gives a basic understanding of the performance of this type of transition.

4 Conclusions

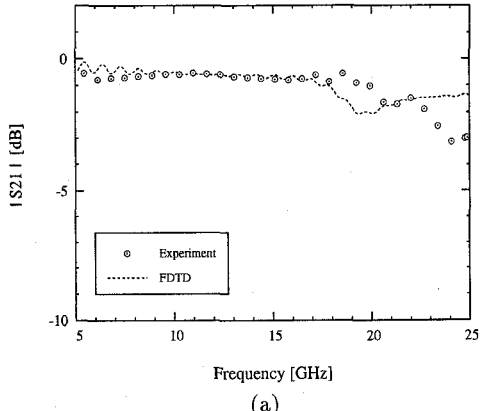
The finite element method (FEM) and the Finite Difference Time Domain (FDTD) technique have been used to characterize hermetic walls commonly found in MIC and MMIC packaging. The derived FEM and FDTD results, as well as measurement agreed very well in low as well as high frequency regions. It was shown that the vias, placed at the grounded CPW to equalize the potential between the ground planes on the upper and lower surfaces, play a key role in the performance of this transition. The hermetic wall placed on top of the CPW transmission line section degrades the return loss of the original circuit only by a couple of dBs. In addition, the hermetic bead transition was found to gradually degrade in performance as frequency increases.

Acknowledgement This research is supported by U. S. Army Research Office and Texas Instruments.

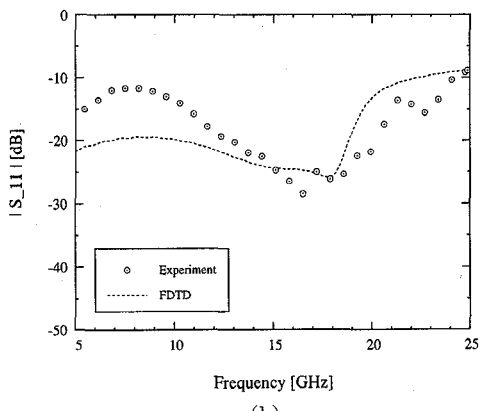
References

- [1] S. Joshi and B. Becker, "Metal Hermetic Surface Mount Packaging," *Microwave J.*, vol. 35, pp. 144-145, July 1992.

- [2] B. Ziegner, "High Performance MMIC Hermetic Packaging," *Microwave J.*, vol. 29, pp. 133-139, Nov. 1986.
- [3] L. Katehi, "The Role of EM Modeling in Integrated Packaging," *1993 IEEE Antennas and Propagation Society Int. Symp. Digest*, vol. 2, pp. 982-985, 1993.
- [4] C. Amrani, M. Drissi, V. Fouad, and J. Citerne, "Packaging and Interconnection Mutual Coupling Effects in Planar Structures and Discontinuities," *1993 IEEE Int. MTT-S Symp. Digest*, pp. 843-846, 1994.
- [5] P. Mezzanotte, M. Mongiardo, L. Roselli, and R. Sorrentino, "FDTD Analysis of High Performance MMIC Package," *1994 IEEE Int. MTT-S Symp. Digest*, pp. 337-340, 1994.
- [6] G. Strauss and W. Menzel, "A Novel Concept for MM-Wave MMIC Interconnects and Packaging," *1994 IEEE Int. MTT-S Symp. Digest*, pp. 1141-1144, 1994.
- [7] M. Rittweger, M. Werthen, and I. Wolff, "3D FDTD Analysis Applied to the Investigation of the Resonant Behavior of Ceramic Feedthrus," *1994 IEEE Int. MTT-S Symp. Digest*, pp. 1719-1722, 1994.



(a)



(b)

Figure 1: Computed and measured S-parameters for open structure without hermetic wall on top and vias under CPW ground. (a) S_{11} . (b) S_{21} . In this case, duroid substrate, which has a relative dielectric constant ϵ_r of 10.8, is used. The CPW ground planes and the PEC underneath the substrate are connected in the measurements. Other geometrical factors are as in Figure 2.

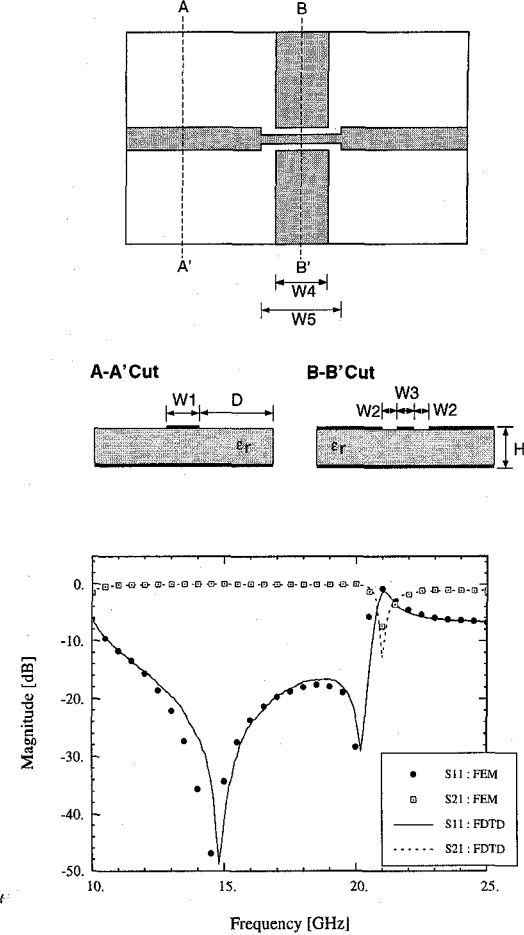


Figure 2: Geometry of the Microstrip-through-CPW transition in a shielded environment and computed results. $W_1 = 0.48$ mm, $W_2 = 0.14$ mm, $W_3 = 0.2$ mm, $W_4 = 2.0$ mm, $W_5 = 3.0$ mm, $H = 0.635$ mm, $\epsilon_r = 12.5$, and $D = 2.26$ mm.

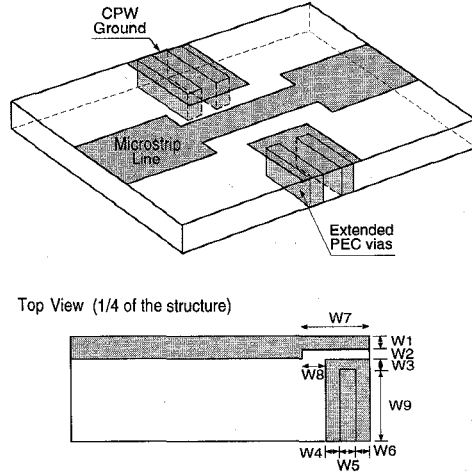


Figure 3 : (continued)

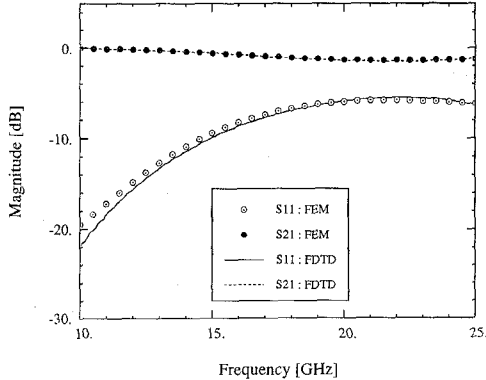


Figure 3: Geometry of the microstrip-through-CPW transition with extended rectangular via hole grounding and computed S-parameters. $W_1 = 0.1$ mm, $W_2 = 0.14$ mm, $W_3 = 0.226$ mm, $W_4 = 0.2$ mm, $W_5 = 0.6$ mm, $W_6 = 0.2$ mm, $W_7 = 1.5$ mm, $W_8 = 0.5$ mm, and $W_9 = 2.034$ mm. The thickness and dielectric constant of the substrate are 0.635 mm and 12.5, respectively.

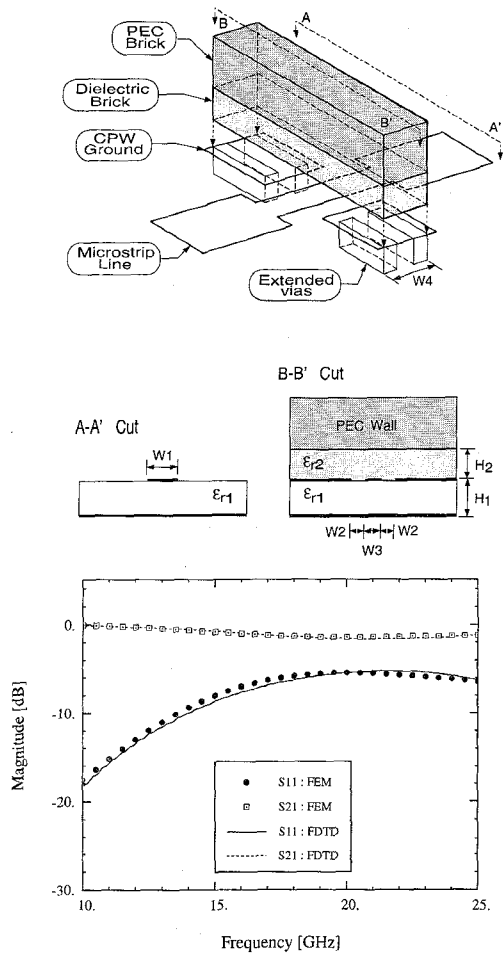


Figure 4: Geometry of the microstrip-through-CPW transition through hermetic wall on top of the extended PEC via grounding structure and computed S-parameters. The width of the hermetic wall is 1.6 mm. $W_1 = 0.48$ mm, $W_2 = 0.14$ mm, $W_3 = 0.2$ mm, $W_4 = 2.0$ mm, $W_5 = 3.0$ mm, $H_1 = H_2 = 0.635$ mm, $\epsilon_{r1} = 12.5$, $\epsilon_{r2} = 2.3$.

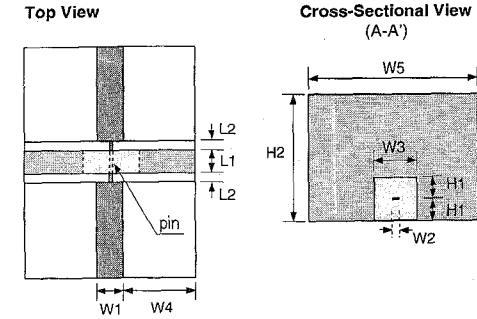
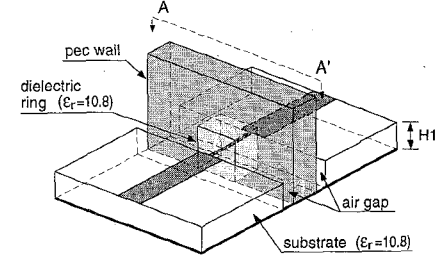


Figure 5: Geometry of the hermetic bead transition and computed scattering parameters. $W_1 = 0.55$ mm, $W_2 = 0.21$ mm, $W_3 = 1.27$ mm, $W_4 = 2.225$ mm, $W_5 = 5.0$ mm, $H_1 = 0.635$ mm, $H_2 = 4.0$ mm, $L_1 = 1.50$ mm, $L_2 = 0.40$ mm, and $\epsilon_r = 10.8$.